Mysteries of PEDESTAL poloidal ASYMMETRIES revealed

Silvia Espinosa and Peter J. Catto

Plasma Science and Fusion Center (PSFC-MIT), Cambridge, USA

Introduction and motivation

Since high confinement operation was discovered, understanding tokamak pedestal physics has become one of the most crucial challenges facing the development of magnetic fusion energy. Gaining insight into flows and transport in this region may lead to the achievement of even higher energy confinement times and, consequently, fusion performance.

It has been suggested that the sudden transition between states of low and high confinement, the L-H transition, involves the suppression of turbulence by sheared radial electric fields [1]. For H-mode pedestals, the amount of turbulence may be only large enough to affect high order phenomena, such as heat transport. Neoclassical collisional theory may than be expected to properly treat low order phenomena, such as flows.

Nevertheless, high confinement mode edge pedestals on Alcator C-Mod [2, 3] (Fig. 1 and 2) exhibit significantly stronger poloidal asymmetry in both boron temperature and density than predicted by the most comprehensive neoclassical theoretical models developed to date [5]. First, the boron temperature is larger on the outboard (LFS) side compared to the inboard side (HFS) by up to a 70%. Hence, it seems not to be a flux surface as assumed by the previous models. Second, there is accumulation of boron density on the high field side up to six fold, which almost doubles the theoretical predictions. Thus, the magnetic field in-out asymmetry seems not to be its only drive. Importantly, the largest in-out asymmetry in density and temperature are not reached at the same radial location (Fig. 2). As a result, there is concern [3] that turbulence might affect even the lowest order phenom-

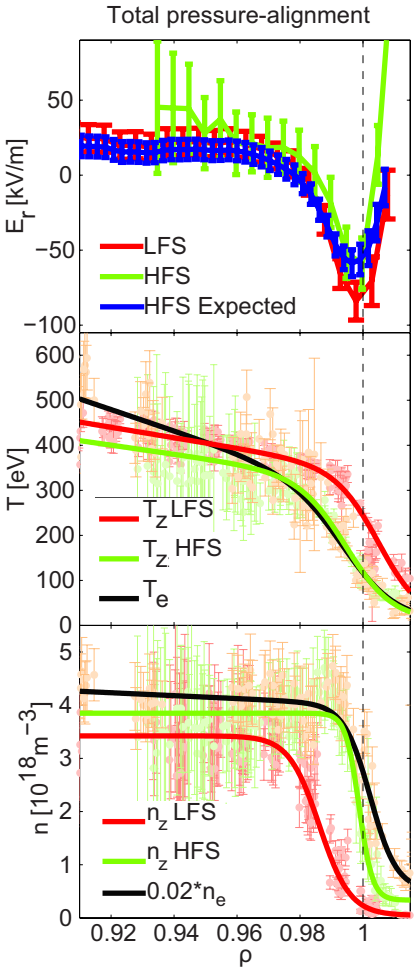

Figure 1: *High and low field side radial profiles of electric field, boron temperature and density [3].*

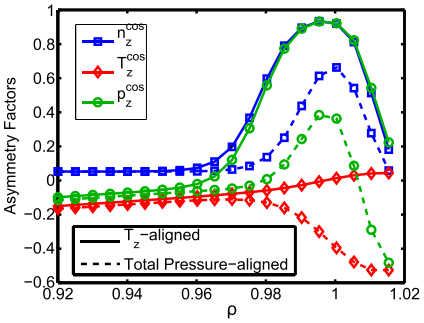

Figure 2: *Experimental in-out asymmetries,* $\frac{HFS-LFS}{HFS+LFS}$ *[3].*

ena, via for instance ballooning modes.

We propose a novel self-consistent neoclassical theoretical model that allows us to explain these poloidal asymmetries, without the need of invoking anomalous transport. Its main novel features are listed on Table 1. First, impurity temperature asymmetries can be driven by inertial effects, which are significant when impurities are allowed to reach sonic speeds. Second, a much stronger impurity density in-out asymmetry than given by just the magnetic field can be introduced by the poloidally varying impurity diamagnetic drift.

Physics captured	[4]	[5]	Us
Non-trace impurities		✓	✓
Strong radial electric field	✓		✓
Diamagnetic flow effects			✓
Strong temperature gradient			✓
Sonic background ions			✓
Poloidal density variation		Weak	✓
Poloidal temperature variation			✓

Table 1: *Physics captured and comparison with previous pedestal models.*

Self-consistent predictive neoclassical model for pedestal poloidal asymmetries

In this section, the novel physics included in the improved neoclassical theory developed and their implications are introduced. The mathematical details will be found in a publication to follow.

Orderings: The theoretical model consists of highly charged non-trace collisional impurities, bulk ions and almost collisionless electrons. Strong impurity temperature and density poloidal variation are allowed. A small aspect ratio limit is assumed, so the poloidal background ion gyroradius is much larger than the ion gyroradius. The pedestal width of electrostatic potential can be comparable to the poloidal background ion gyroradius, so that the impurity and background ion flows can reach the ion thermal speed. In addition, the pedestal width of the impurity density is such that the impurity diamagnetic drift contribution is allowed to be comparable to the impurity poloidal and toroidal flow terms when measuring the radial electric field, as experimentally observed [2]. Sonic behavior is assumed to happen for the background ion diamagnetic term. The bulk ion temperature pedestal width is taken to be of the same order as that of its density. Finally, it is assumed that the impurity and background ion temperatures are of the same order at all pedestal radial locations, and hence its

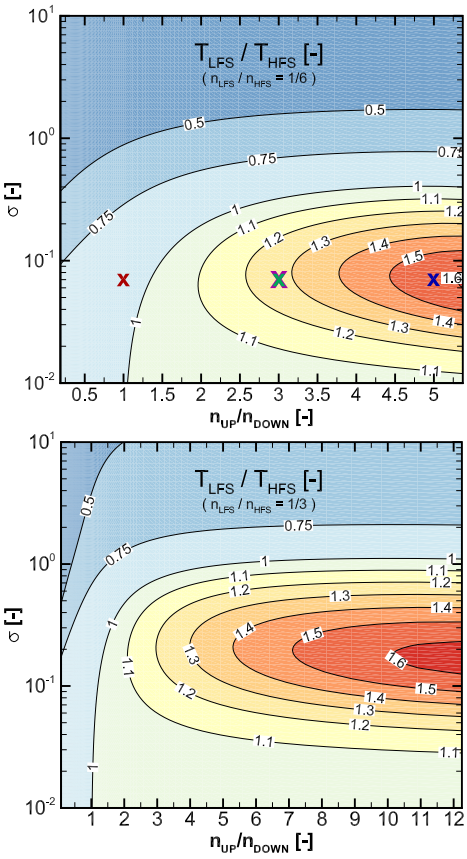

Figure 3: *Effect on the ratio of outboard to inboard impurity temperature of the impurity density up-down asymmetry and ratio between poloidal and collisional impurity flow, σ. Both strong (up) and weak (down) impurity density in-out asymmetry are presented.*

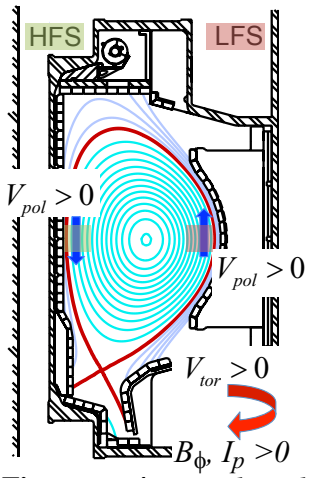

Figure 4: *Tokamak poloidal cross section [2].*

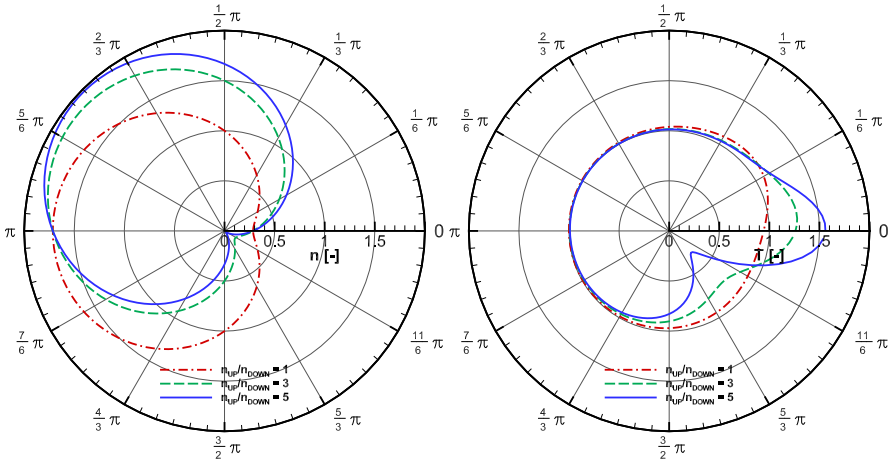

Figure 5: *Dimensionless impurity density (left) and temperature (right) polar profiles, for points marked on Fig.3.*

pedestals widths are of the same order. As a result, the impurity density pedestal width is smaller than that of its temperature by approximately the ratio of impurity to background atomic numbers, which is also in agreement with the experiments (Fig. 1).

Conservation equations for impurities: In order to analyse the parallel dynamics on each flux surface separately, the parallel equilibrium is assumed to be reached much faster than the cross field equilibrium. The perpendicular momentum conservation is assumed to be given by

$$\mathbf{V}_{z\perp} = \frac{c}{B^2}\mathbf{B}\times\left(\nabla\Phi + \frac{1}{z_z e n_z}\nabla p_z\right) \tag{1}$$

where $\mathbf{V}_z$ is the impurity flow, $\mathbf{B}$ is the magnetic field, Φ the electrostatic potential and z_z, n_z and p_z the impurity atomic number, density and pressure, respectively. Using conservation of particles on the flux surface,

$$\mathbf{V}_z = -cR^2\nabla\zeta\left(\frac{\partial\Phi}{\partial\psi} + \frac{1}{z_z e n_z}\frac{\partial p_z}{\partial\psi}\right) + \frac{K_z}{n_z}\mathbf{B} \tag{2}$$

where R is the tokamak major radius, ζ and ψ the poloidal angle and flux and K_z a flux function.

The parallel momentum and energy conservation equations are assumed to be the following:

$$m_z n_z \mathbf{V}_z\cdot\nabla\mathbf{V}_z\cdot\frac{\mathbf{B}}{B} = R_{zi\|}, \qquad R_{zi\|} = \frac{1}{2}m_z n_z \nu_{zi}\left(V_{i\|} - V_{z\|}\right) + O\left(\sqrt{\varepsilon}\right) \tag{3}$$

$$\frac{n_z^2}{T_z^{\frac{1}{2}}}\mathbf{V}_z\cdot\nabla\left(\frac{T_z^{\frac{3}{2}}}{n_z}\right) = Q_{zi}, \qquad Q_{zi} = \frac{3}{2}n_z\nu_{zi}\left(T_i - T_z\right) + O\left(\sqrt{\varepsilon}\right) \tag{4}$$

where m_z is the impurity mass and ν_{zi} the collision frequency of bulk ions and impurities, $V_{i\|}$ the bulk ion parallel flow, ε the aspect ratio and T_z and T_i the impurity and bulk ion temperatures.

Conclusions

Given an impurity density profile, such us $n \approx 1 + C\cos\theta + S\sin\theta$, the energy equation can be solved numerically for the impurity temperature (Fig. 3); where $n \equiv \frac{n_z}{\langle n_z\rangle}$, $T \equiv \frac{T_z}{T_i}$, $\sigma \equiv \frac{K_z\mathbf{B}\cdot\nabla\theta}{\nu_{zi}\langle n_z\rangle} \sim$

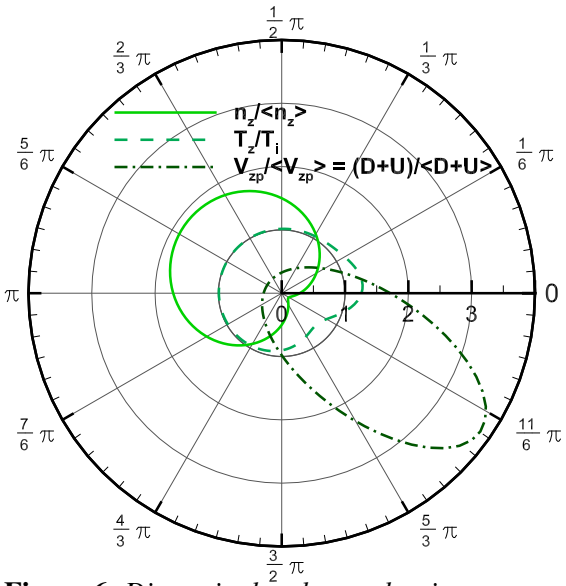

Figure 6: *Dimensionless boron density, temperature and poloidal velocity polar profiles, for the green point marked on Fig.3.*

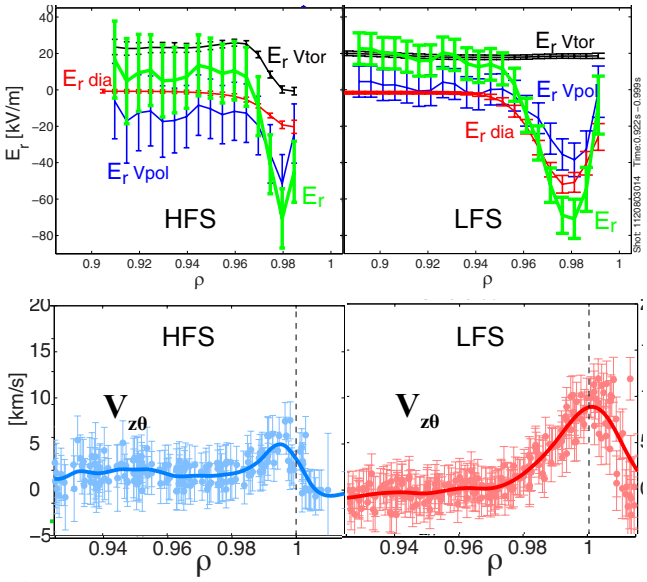

Figure 7: *Inboard (left) and outboard (right) radial profiles of the radial electric components [2] (top) and boron poloidal flow (down) [3].*

$\frac{V_{zp}}{\nu_{zi} q R}$, θ the poloidal angle and $\langle\rangle$ denotes flux surface average. It can be seen that, in the small aspect ratio limit, the model developed can capture the experimental temperature by selecting appropriately the up-down asymmetry of the density (Fig. 3 and 5).

When the bulk ion density and temperature vary slowly poloidally, the parallel momentum equation has an analytical solution given by $n = \frac{1}{D+U} + O\left(\sqrt{\varepsilon}\right)$; where $U \equiv \frac{B V_{\|i} \langle n_z \rangle}{K_z \langle B^2 \rangle} \sim \frac{V_{\|i}}{V_{z\theta}}$ and $D \equiv \frac{c \langle n_z \rangle \sqrt{\langle R^2 \rangle}}{K_z \sqrt{\langle B^2 \rangle}} \left(\frac{\partial \Phi}{\partial \psi} + \frac{1}{z_z e n_z} \frac{\partial p_z}{\partial \psi} \right) \sim \frac{V_{z\zeta}}{V_{z\theta}}$. It can be solved for the poloidal variation of the impurity diamagnetic flow, which is similar to that of the impurity poloidal flux (Fig. 6). These predictions successfully agree with the experiments (Fig. 7). Hence, this theory may be used in the future to get information, for instance, about all poloidal angles or the background.

We conclude that these extensions in neoclassical theory successfully capture the strong experimental poloidal impurity temperature and density variation, providing a more realistic predictive model for pedestal observations without the need of invoking anomalous transport.

References

[1] J.W. Connor and H.R. Wilson, Plasma Phys Contr Fusion **42**:R1 (2000)

[2] C. Theiler et al., Nucl Fusion **54**, 083017 (2014)

[3] R.M. Churchill et al., Phys.Plasmas, **22**, 056104 (2015)

[4] G. Kagan and P.J. Catto, Plasma Phys Contr Fusion **50**, 085010 (2008)

[5] P. Helander, Phys Plasmas **5**, 3999 (1998)

The authors are indebted to Prof. Ian Hutchinson and Jeffrey Freidberg for stimulating discussions.Work supported by DOE Grant DE-FG0291ER54109 and La Caixa Fellowship.